ISSN: 2449 – 0539
BAYERO JOURNAL OF ENGINEERING AND TECHNOLOGY (BJET) VOL.16 No.3, AUGUST, 2021 PP 65 - 70

PD FAST FRACTIONAL TERMINAL SLIDING MODE CONTROL FOR TRAJECTORY TRACKING

Zulfiqar I. Bibi Farouk

Mechanical Engineering Department, Tianjin University, Tianjin, 300350, China

ABSTRACT

This study describes a noble design of a sliding mode controller for a fast fractional terminal sliding mode to handle the speed and position of a 2-Dof robot. The sliding surfaces utilized in the study used a PD controller in a commonly used teminal sliding mode control to identify discrepancies that were highly influenced by the Coriolis effect. The new control law benefits from the simplicity and ease of construction of PD control as well as the resilience of terminal sliding mode control to model uncertainty and parameter variation. To prevent amplifying the control signals if the signals remained fixed and high for the time being, the PSO algorithm was employed to estimate and modify the control parameters. The obtained results demonstrate that the proposed technique is superior at all costs.

Keywords: Fast fractional terminal sliding mode control; Particle swarm optimization; Perturbation; fitness error; Biopsy robot.

1. INTRODUCTION

Proportional integral differential (PID) is a traditional control approach that is still frequently used today in many innovations because of its simplicity and applicability. However, if the plant is nonlinear, performance reduces as the controllers are not ideal in system stabilization, especially where nonlinearity is high or the uncertainty bound is enormous. Many practical situations need perfect control performance that rebuffs disturbances and trails the desired trajectory. A dynamical system whose form varies depending on the current value of its state is known as a variable structure system (VSS). A VSS may be considered as a collection of independent structures (continuous subsystems) linked together by a switching logic. It may leverage the desired features of each of the structures that make up the system by using a suitable switching method. This makes its control strategies discontinuous functions of state variables, perturbations, and reference inputs. Sliding modes play the dominating role in VSS theory, and the basic notion of creating VSS control algorithms relies on enforcing sort of motion in specific sliding surfaces in the system state spaces.

Because of the robustness features of SMC, the technique has become an intensely popular and appropriate method for controlling a wide range of linear and nonlinear systems. In the face of external disturbances and uncertainties, sliding mode control (SMC) excels due to its insensitivity. An SMC is built to force system trajectories into a predetermined manifold in a specific fixed time and reach an equilibrium point on the surface (Zebardast and Ghadiri, 2013). The SMC switching function laws completely govern the system's closed-loop dynamics as long as the system trajectories stay on this surface. Numerous SMC techniques involving theoretical development and implementation have emerged over time.

The common flaw of any SMC, terminal or otherwise, is control signal high-frequency oscillation tied to the discontinuity feature of the control method. In (Moldoveanu, 2014) two major reasons were outlined: firstly, the fast dynamics in the control loop were disregarded during system design (modeling), and secondly, fixed sampling rates were used in microcontrollers.

Many researchers proposed different control methods. Majority of the controllers has perfect tracking performance in theory but it is not practically applicable. This lead the author of this work to proposed a robust practically applicable controller that avoid/minimize high frequency oscillation.

The paper has two distinctive contributions. Firstly, it presented a robust hybrid controller based on a novel fast fractional terminal sliding mode control (FFTSMC), taking advantage of the superiority of terminal sliding mode control (TSMC) over standard SMC. The proposed method in this study distinguishes itself by employing a PD controller in a widely used TSMC to detect discrepancies heavily contributed by the Coriolis effect. Lastly, particle swarm optimization (PSO) is applied to optimize the system control parameters if certain criteria are fulfilled, which is explained in section 2 under the subheading PSO.

2. DYNAMIC MODEL

The universal derived dynamic equation for the serial manipulator and other machines is given in equation (1).

$$M(q)\ddot{q} + C(q,\dot{q})\dot{q} + G(q) + F_r + T_d = \tau \quad \ldots \quad (1)$$

where $\ddot{q}, \dot{q}, q \in R^n$ are the joints input vectors of acceleration, velocity, and position, respectively. $M(q) \in R^{nxn}$ is the inertia matrix which assumes to be symmetric and positive definite, $C(q,\dot{q}) \in R^n$ are the Coriolis and centrifugal term, $G(q) \in R^n$ is the gravitational torque vector, $F_r \in R^n$ is the friction effect, $T_d \in R^n$ is unknown but bounded disturbances, and τ is the applied joint torque.
Equation (1) can be written as;

$$\ddot{q} = M^{-1}\tau - M^{-1}C\dot{q} - M^{-1}G - M^{-1}F_r - M^{-1}T_d \quad \ldots \quad (2)$$

A biopsy intended robot of 2-Dof (see Fig. 1) is designed to validate the proposed method. The closed dynamics equations of the device is given in the appendix.

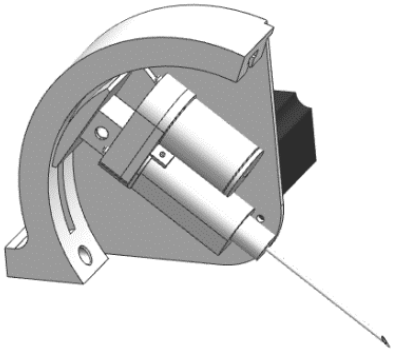

Fig. 1. Biopsy mechanism of 2-DoF.

Broadly speaking, LSMC is widely used to controlled robotics systems for quite being (Rahmani and Rahman, 2020), this is due to its property mentioned earlier (Zhao et al., 2008). Categorically, the application of TSMC surpasses the traditional SMC in many aspects (Zhao et al., 2009). It is crucial when dealing with SMC of any kind to choose an appropriate sliding surface in order to have reasonable control. The proposed sliding surface in this research is composed of nonlinear fractional-order, as shown in equation (3).

$$s(t) = K_d\dot{e} + K_p e + n\lambda(|e|^{\alpha} sign(e)) \quad \ldots \quad (3)$$

The errors $\dot{e}$ *and* e converges to zero in finite time at all given initial states by employing the appropriate controller. The order of the fractional gain is α = p/q, where both $p,q > 0$ and positive odd numbers such that $p<q<2p$. Likewise, the gain parameter $\lambda > 0$ is in the range [0.01,1] and n any arbitrary number greater than zero. The tracking errors are $e = q_d - q, \dot{e} = \dot{q}_d - \dot{q}$ *and* $\ddot{e} = \ddot{q}_d - \ddot{q}$.

The equivalent controller can be realized as;

$$\dot{s}(t) = K_d\ddot{e} + K_p\dot{e} + \alpha n\lambda|e|^{\alpha-1} sign(e) \quad \ldots \quad (4)$$

Further simplification of (4) yields to

$$\dot{s}(t) = K_d(\ddot{q}_d - \ddot{q}) + K_p\dot{e} + \alpha n\lambda|e|^{\alpha-1} sign(e) \quad \ldots \quad (5)$$

Substituting (2) into (6) produce;

$$\dot{s}(t) = K_d\left(\ddot{q}_d - M^{-1}(\tau - C\dot{q} - G - F_r - T_d)\right) + K_p\dot{e} + \alpha n\lambda|e|^{\alpha-1} sign(e) \quad \ldots \quad (6)$$

In view of τ as the control variable, the equivalent control is derives as;

$$U_{eq} = M(\ddot{q}_d) + C\dot{q} + G + F_r + T_d + \frac{M}{K_d}\left(K_p\dot{e} + \alpha n\lambda|e|^{\alpha-1} sign(e)\right) \quad \ldots \quad (7)$$

The controller in (7) above will not achieve asymptotic exponential trail of the required close-loop output due to disturbances, perturbation and parameter variation (Rahmani et al., 2020). Some of the discrepancies a heavily contributed not only from external disturbances but from reaction forces in the joints better known as coriolis and centrifugal effects. Consequently, another controller is added to further suppress the unwanted effects and to match up the reaching condition perfectly in the presence of disturbances in the desired input.

$$U = U_{eq} + U_s \quad \ldots \quad (8)$$

To verify the stability of the controller, a Lyapunov function candidate is considered.

$$L(t) = \frac{1}{2}s(t)^T s(t) \quad \ldots \quad (9)$$

Taking the derivatives of (9) and substituting (6) in it, and then replacing the τ with (8) the new equation yields;

$$\dot{L}(s) = s^T \left(K_d \left(\ddot{q}_d - M^{-1}\left(U_{eq} + U_s - C\dot{q} - G - F_r - T_d\right)\right) + K_p\dot{e} + \alpha n\lambda |e|^{\alpha-1} sign(e) \right) \quad \dots \quad (10)$$

Putting the equivalent controller (7) in equation (10) and simplify further, leads to;

$$\dot{L}(s) = -s^T U_s \quad \dots \quad (11)$$

Evidently, equation (11) is less than zero, the feedback controller is selected as a combination of equivalent and reaching controllers. Reaching control signal help in achieving the desired control perfectly. We give preference to the deflection occurred when one robot link is revolving above another rotating link (Thomas, 2016), which results in coriolis. This effect is part of unmodeled dynamics parameters, which might lead to nonvanishing perturbations. With that, the reaching control law is chosen to be a saturation function to avoid chattering.

$$U_s = \text{sat(s)} = \begin{cases} -1, & \text{s} < -\eta \\ 1, & \text{s} > \eta \\ \text{Ks}, & |s| \le \eta, \quad \text{K} = \frac{1}{\eta} \end{cases} \quad \dots \quad (12)$$

The diagonal matrices k_p, k_d, λ, n, α, of the control gains if were remained high and fixed for some time might amplify the control signal oscillation and leads to the system of high-frequency unmodeled dynamics (Li and Xu, 2010). Therefore, there is a need to tune the control gains to avoid such unnecessary oscillations and keep the sliding surface on or quasi zero.

The best way to tune the parameters is to employ an optimization toolbox. Moreover, we proposed to use the improved particle swarm optimization (PSO) in (Umar et al., 2020), due to the fact of fast convergence. Another things with PSO is, every particle is connected within the Swarm, this helps in sharing information for search direction which might be the reason for quick convergence and stagnation in SPSO (Umar et al., 2020).

2.1. Particle Swarm Optimization

The algorithm begins by setting n-random particles with m-dimensions. The particles (birds or fishes) position X_i and velocity V_i is given by;

$$\begin{cases} X_i = (x_{i1}, x_{i2}, \dots, x_{im}), \\ V_i = (v_{i1}, v_{i2}, \dots, v_{im}), \end{cases} \quad \dots \quad (13)$$

For every iteration, the position and velocity of the i-particle is updated according to equation (14) (Umar et al., 2020).

$$\begin{cases} V_{i(t+1)} = wrV_{i(t)} + c_1 r_1\left(P_{ibest}(t)\right) - X_{i(t)} \\ \qquad +c_2 r_2\left(G_{ibest}(t) - X_{i(t)}\right) \\ X_{i(t+1)} = X_{i(t)} + V_{i(t+1),} \end{cases} \quad \dots \quad (14)$$

Given that $P_{ibest} = (p_{ibest}, p_{ibest}, \dots, p_{ibest})$ and $G_{ibest} = (g_{ibest}, g_{ibest}, \dots, g_{ibest})$, w is the inertia weight, while c_1 and c_2 is the learning coefficient. The coefficient r is numbers generated randomly between [0,1]. The major characteristic of good PSO is the balance between exploration, exploitation and avoiding stagnation, but this need a prior knowledge of well-established w and c. This can be achieve by tuning the PSO parameters, to achieve that we adopted the used of non-linear decreasing w and increasing c in our previous work (Umar et al., 2020).

$$\begin{cases} w_{iter} = w_{initial} \times n^{iter} \\ c_1 = 2.24 \\ c_2 = \frac{c_{initial}}{m^{iter}} \end{cases} \quad \dots \quad (15)$$

here, n and m variables depend on the problem to solve.

Fitness function selection has an enormous effect on the tune parameters (Li and Xu, 2010). In this research, we proposed the fitness function as follows:

$$f(K_p K_d \lambda \alpha n) = (e_i \dot{e}_i)^2 \quad \dots \quad (16)$$

The stopping criteria are based on mutation function in which if the solution is stagnant at local minima, the function pushes it out. Variables and conditions were used to train the function to find the stagnant point.

The fitness error f_e given in (17), is the difference between the current and previous fitness.

$$\boldsymbol{f_e = fitness_{t-1} - fitness_t} \quad \dots \quad (17)$$

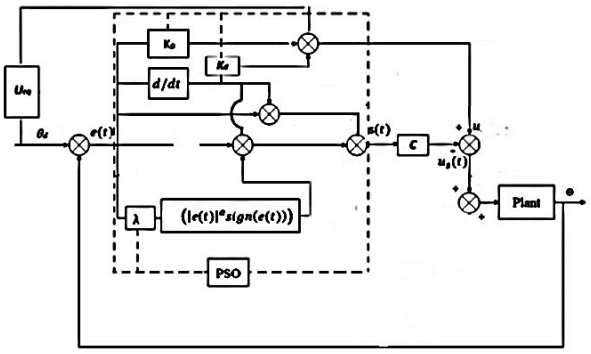

Fig. 2. Proposed control method block diagram.

3. SIMULATION AND DISCUSSION

The dynamics parameters given in table 1 are used with a 2-DoF biopsy mechanism stated early to conduct a simulation in matlab environment to verify our proposed method. We compared the results obtained with the TSMC given in equation (18). To be fair with the obtained results using TSMC, we employed the same optimization procedure to tune all the required control parameters involve

$$s(t) = \dot{e} + \lambda_1 e + \lambda_2(|e|^{\alpha} sign(e)) \quad \ldots \quad (18)$$

Table 1: The robot parameters.

S/N.	Simulation parameter	Link 1	Link 2
1	Mass (Kg)	1	1.5
2	Length (m)	0.5	0.8
3	Inertia (Kgm^2)	0.5	5
4	Joints initial inputs (rad, rad/s)	0,0	0,0

The desired signals are $q_{d1} = 6\sin t + 0.3\cos t$, $q_{d2} = 6\sin t + 0.3\cos t$. A threshold was set to the sliding surface to avoid unnecessary tuning. As such, it is not continuous tuning unless it is required. This also facilitates the speed of the outcomes. The PSO parameters used in the simulation are, $n = rand(2,1), 1 \le m \le 2.24$, $w_{ini} = (0.2,0.2)$ Depicted in Fig. 3 is the tracking control of joints position under the proposed method FFTSMC and TSMC. It demonstrates the efficiency of the proposed method over the counterpart approaches in trailing the reference trajectory and speed of convergence.

The joints position's tracking error is depicted in Fig. 4; although both results demonstrate good performance, FFITSMC outperformed the ordinary TSMC with the least trailing error. This also shows that there is apparently zero overshoot or undershoot in the joints position tracking for the proposed method.

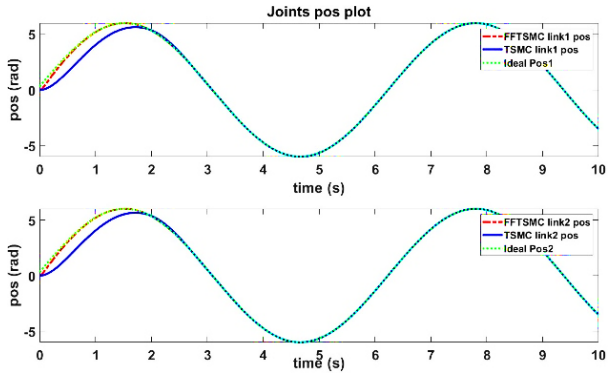

Fig. 3 Joints position under FFTSMC and TSMC both tune with improve PSO algorithm.

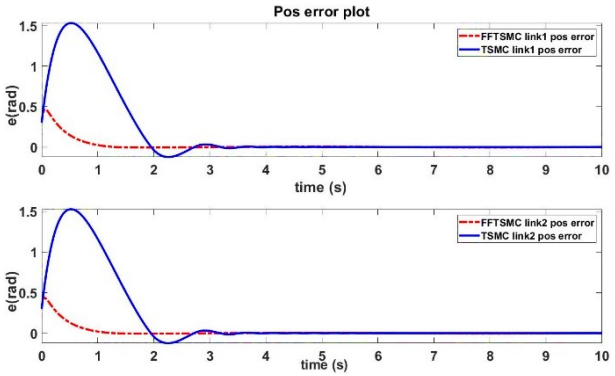

Fig. 4. Joints position errors under FFTSMC and TSMC both tune with improved PSO algorithm.

In Fig. 5 and 6, the joint velocity control demonstrates the proposed method's superior performance and efficiency over TSMC. The system internal perturbation due to Coriolis and other effects were significantly suppressed, this shows the robustness of the proposed controller.

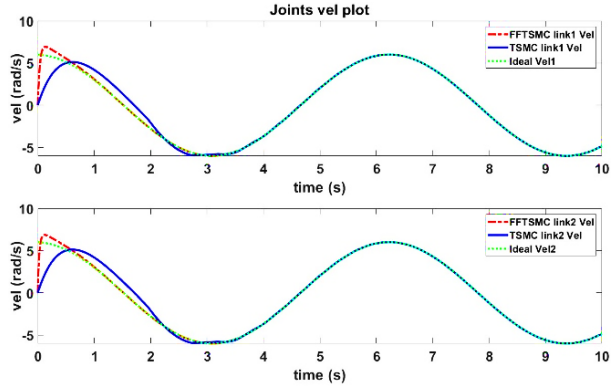

Fig. 5. Joints velocity under FFTSMC and TSMC both tune with improved PSO algorithm.

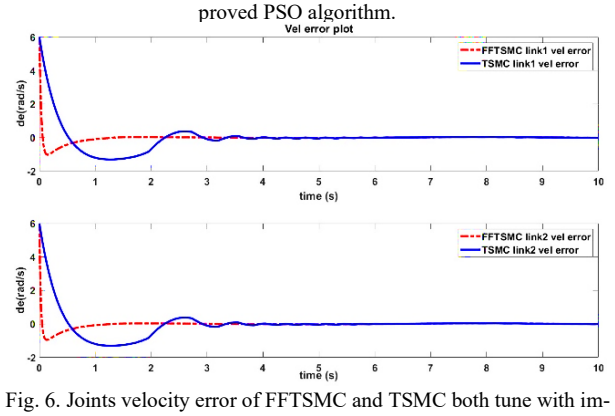

Fig. 6. Joints velocity error of FFTSMC and TSMC both tune with improved PSO algorithm.

To further verify the robustness, we introduced a random noise to the control input.

$$\delta(t) = 0.1 * rand(1,1) \quad \ldots \quad (20)$$

Fig. 7 shows the joint's position and velocity error tracking performance with random noise. We observed that the convergence speed is also attributed to the complexity of the desired control input.

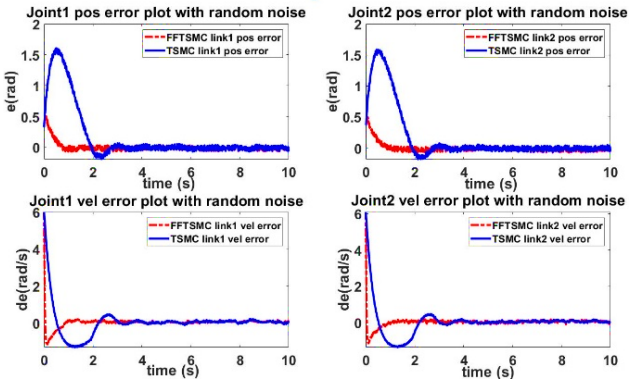

Fig. 7. Joints position and velocity error of FFTSMC and TSMC under random perturbation both tune with the PSO.

The switching surface plot is presented in Fig. 8, this authenticates the intense of the system sensitivity and the ability to correct the system error early. In cognisance with Fig. 9, the starting input torque is less in FFITSMC than in TSMC, this is another added advantage to of the hybrid proposed control. The controllers in both cases demonstrated an excellent ability to suppress the external perturbation. However, there exist a clear indication that FFITSMC has a superior ability to maintain fast convergence and tracking ability.

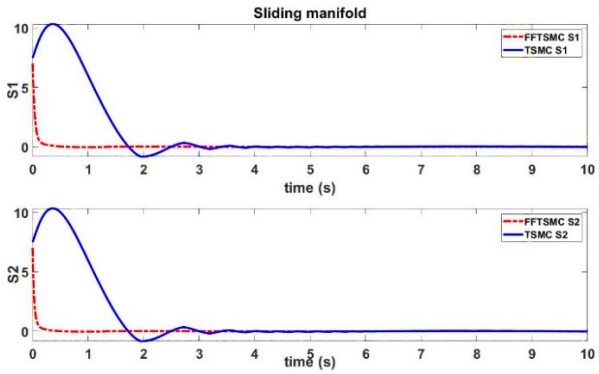

Fig. 8. Sliding surface under FFTSMC and TSMC both tune with improve PSO algorithm.

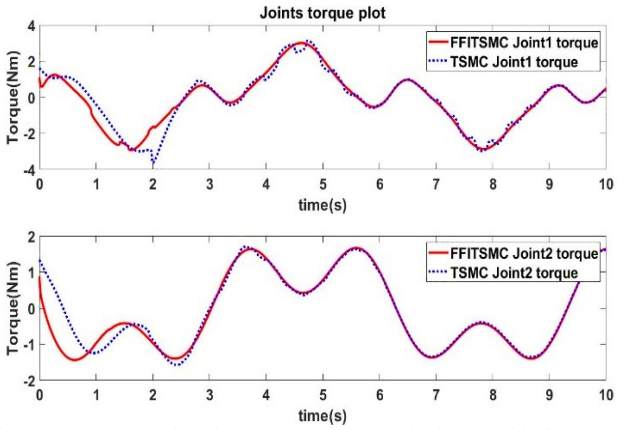

Fig. 9. Joints torque plot of FFTSMC and TSMC both tune with the PSO algorithm.

3.1. Conclusion

This paper proposed a new approach for fast fractional terminal sliding mode control, simulated with a 2-DOF biopsy mechanism. The chattering created due to the fast fractional term in the controller and the external disturbances are eliminated successfully. The unmodeled and neglected dynamics terms, unknown but bounded disturbances, are address by adding the PD controller to the main fast fractional controller. The PD term stabilizes the system by giving early corrective feedback for the slightest error signal. The gains matrices are tuned with the PSO optimization algorithm to avoid amplifying the control signals if they were fixed and remain high for the time being. The method's performance is compared with TSMC, in which PSO algorithms were also used to tunes the control parameters.

APPENDIX

$$\tau = \begin{bmatrix} \tau_1 \\ \tau_2 \end{bmatrix} \quad \ldots \quad (a)$$

$$M(q) \begin{bmatrix} \frac{m_1 a_1^2}{4} + m_2 d_2^2 + m_2 l_2 a_1 + \frac{m_2 a_1^2}{4} + l_1 + l_2 & 0 \\ 0 & m_2 \end{bmatrix} \quad (b)$$

$$C(q,\dot{q}) = \begin{bmatrix} \left(m_2 d_2 + \frac{m_2 l_1}{2}\right)\dot{d}_2 & \left(m_2 d_2 + \frac{m_2 l_1}{2}\right) \\ \left(-m_2 d_2 + \frac{m_2 l_1}{2}\right)\dot{\theta}_1 & 0 \end{bmatrix} \quad (c)$$

$$\dot{\theta} = \begin{bmatrix} \dot{\theta}_1 \\ \dot{\theta}_2 \end{bmatrix} \quad \ldots \quad (d)$$

$$G(q) = \begin{bmatrix} \frac{m_1 g l_1 cos\theta_1}{2} + m_2 g\,(\frac{l_1}{2} + d_2)\cos\theta_1 \\ m_2 \sin(\theta_1) \end{bmatrix} \quad \ldots \quad (e)$$

$$\theta = \begin{bmatrix} \theta_1 \\ \theta_2 \end{bmatrix} \quad \ldots \quad (f)$$

4. REFERENCES

Li, Y. and Xu, Q. (2010). Adaptive sliding mode control with perturbation estimation and PID sliding surface for motion tracking of a piezo-driven micromanipulator. IEEE Transactions on Control Systems Technology Vol. 18 No. 4: pp.798-810.

Moldoveanu, F. (2014). Sliding mode controller design for robot manipulators. Bulletin of the Transilvania University of Brasov. Engineering Sciences., Series I Vol. 7 No. 2: pp.97.

Rahmani, M., Komijani, H. and Rahman, M. H. (2020). New Sliding Mode Control of 2-DOF Robot Manipulator Based on Extended Grey Wolf Optimizer. International Journal of Control, Automation and Systems, Vol. 18 No. 6: pp.1572-1580.

Rahmani, M. and Rahman, M. H. (2020). Adaptive Neural Network Fast Fractional Sliding Mode Control of a 7-DOF Exoskeleton Robot. International Journal of Control, Automation and Systems Vol. 18 No. 1: pp.124-133.

Thomas, P. P. (2016). The Analysis of Coriolis Effect on a Robot Manipulator. International Journal of Innovations in Engineering and Technology (IJIET) :pp.370-375.

Umar, A., et al., (2020). Developing a new robust swarm-based algorithm for robot analysis. Mathematics, Vol. 4 No. 2.

Zebardast, A. and Ghadiri, H. (2013). DC Motor Control Using Sliding Mode Method. Electr. Comput. Eng, Vol. 7.

Zhao, D., Li, S. and Gao, F. (2008). A new terminal sliding mode control for robotic manipulators, Vol. 41 No. 2: pp.9893,

Zhao, D., Li, S. and Gao, F. (2009). A new terminal sliding mode control for robotic manipulators. International Journal of control, Vol. 82 No. 10: pp.1813,